Eur. Phys. J. C 17, 121–128 (2000)
Digital Object Identifier (DOI) 10.1007/s100520000429

THE EUROPEAN PHYSICAL JOURNAL C

An estimate of higher twist at small $x_{\rm B}$ and low Q^2 based upon a Saturation Model*

J. Bartels[1,a], K. Golec-Biernat[1,2,b], K. Peters[1,c]

[1] II. Institut für Theoretische Physik, Universität Hamburg, Luruper Chaussee 149, 22761 Hamburg
[2] Institute of Nuclear Physics, Radzikowskiego 152, 31-342 Krakow, Poland

Received: 20 March 2000 / Published online: 9 August 2000 – © Springer-Verlag 2000

Abstract. We investigate the influence of higher twist corrections to deep inelastic structure functions in the low-Q^2 and small-x HERA region. We review the general features of the lowest-order QCD diagrams which contribute to twist-4 at small-x, in particular the sign structure of longitudinal and transverse structure functions which offers the possibility of strong cancellations in F_2. For a numerical analysis we perform a twist analysis of the saturation model which has been very successful both in describing the structure function and the DIS diffractive cross section at HERA. As the main conclusion, twist 4 corrections are not small in F_L or F_T but in $F_2 = F_L + F_T$ they almost cancel. This indicates the limitation on the use of the DGLAP formalism at small x and Q^2. We point out that F_L analysis needs a large twist-4 correction. We also indicate the region of validity of the twist expansion.

1 Introduction

A deeper understanding of the transition from perturbative QCD to nonperturbative Pomeron physics in deep inelastic scattering at low Q^2 and small x remains one of the central tasks in HERA physics. Approaching the transition region from the perturbative side, one expects to see the onset of large perturbative corrections - in particular those which belong to higher twist operators in QCD. The twist expansion defines a systematic approach and, therefore, provides an attractive framework of investigating the region of validity of the leading-twist NLO DGLAP evolution equations. The essentials of the theory of higher twist operators and their Q^2-evolution have been laid down twenty years ago: a choice of a complete operator basis has to be made [1], and for the evolution [2] one needs to compute evolution kernels which, for partonic operators in leading order, reduce to $2 \to 2$ kernels. The problems of mixing between different operators of a given twist has also been addressed in [2]. Explicit calculations have been done mainly for fermionic operators. In the small-x region at HERA, however, we expect gluonic operators to be the most important ones. Recently, a first attempt has been carried out to analyze the twist-4 gluonic operators in the double-logarithmic approximation (DLA) [3,4]. In addition to analytic calculations also a first numerical analysis has been presented. As one of the main results, it has been pointed out that, due to a complicated sign structure, subtle cancellations among different twist-4 corrections are possible. As to the numerical results, the freedom in choosing initial conditions for twist-4 gluonic operators, in combination with our presently very limited knowledge of the twist-4 evolution equations, make a systematic QCD study of higher twist corrections in the low-Q^2 and small-x region at HERA a rather difficult but challenging task.

In order to gain a detailed insight into the role of higher twist it may be helpful to discuss in some detail the simplest low-order QCD-diagrams (rather than using the whole Q^2-evolution machinery collected in [3]). Particular attention has to be given to the question of possible cancellations between different contributions. As to the choice of input distributions, it seems advisable to make use of more specific, model dependent assumptions on the input distribution. The most reasonable starting point, in our opinion, is that model which has been most successful in describing the low-Q^2 data of HERA: the saturation model of [6] which contains only four free parameters. This model not only describes very well the $\gamma^* p$-cross section in the low Q^2 transition region where the role of higher twist is of particular importance, but also allows to connect, in a quantitative way, the total cross section data with the DIS inclusive diffractive process [7]. A particular benefit of using this model is the interpretation in terms of QCD diagrams: comparing with the analysis of the QCD diagrams it is possible to read off a choice of twist-four initial conditions. Since the model (before doing any twist

* Supported by the TMR Network "QCD and Deep Structure of Elementary Particles" and by the KBN grant No. 2P03B 089 13. One of us (K.G.-B.) is supported by *Deutsche Forschungsgemeinschaft*

[a] e-mail: bartels@x4u2.desy.de
[b] e-mail: krzysztof.golec-biernat@desy.de
[c] e-mail: krisztian.peters@desy.de

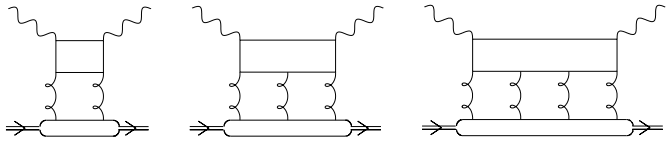

Fig. 1a–c. The simplest QCD diagrams with 2,3 or 4 t-channel gluons

expansion) describes the HERA data, it is also likely to provide a realistic estimate of twist-4 contribution in the low-Q^2 and small-x region.

We begin with reviewing the expressions for the simplest QCD diagrams and discussing patterns of possible cancellations. In the following part we review the saturation model and define the twist expansion. In the third part we perform a numerical analysis and draw our conclusions on the magnitude of gluonic twist-4 corrections. The results of our analysis are in qualitative agreement with the estimates presented in [10], suggesting that twist-4 corrections to $F_2 = F_T + F_L$ are small down to $Q^2 \sim 1$ GeV^2, $x \sim 10^{-4}$. However, we also find that this smallness is due to an almost complete cancellation of the twist-4 corrections to F_T and F_L: both of them, individually, are large, but have opposite signs and nearly the same magnitude. We interpret this as a warning against using the twist-2 formalism at too low Q^2 and small x.

2 QCD Diagrams

We are interested in twist-4 corrections ΔF_i to the transverse (T) and longitudinal (L) structure functions

$$F_i(x,Q^2) = F_i^{\tau=2}(x,Q^2) + \Delta F_i(x,Q^2)\,, \quad i = T, L. \quad (2.1)$$

A QCD analysis of twist-4 corrections at small-x starts from the lowest order diagrams shown in Fig. 1. The photon can have transverse or longitudinal polarization. Approximate expressions for the fermion loop, $D_{4;0}^{(T,L)(abcd)}$ can be found in [3]: they are valid for small x, and corrections are of the order $O(x)$. The diagrams with two gluons start with leading twist, but they also contain higher twist - similar to the BFKL approximation which also contains corrections of all orders in $1/Q^2$. Unfortunately, we have no way to obtain information on the higher-twist couplings to the proton. The diagrams with three gluons, through the reggeization of the gluon, are higher order corrections to the diagram with two gluons; in the analysis of [4] they are needed to complete the covariant derivative of the two gluon diagram. In a complete twist-4 analysis these diagrams with two and three t-channel gluons have to be included, but presently we do not know how to estimate their magnitude. The most interesting twist four diagrams, presumably, are the ones with four gluons. They belong to the four gluon operator which is expected to play the most crucial role at low Q^2 and small x. Its coupling to the proton has been discussed in [3], where arguments have been given that the simplest model which respects the AGK cutting rules consists of (at least) two pieces:

$$\varphi_4^{abcd} = \varphi_{4\mathrm{S}}^{abcd} + \varphi_{4\mathrm{A}}^{abcd} \quad (2.2)$$

where

$$\varphi_{4\mathrm{S}}^{abcd} = \frac{1}{3\cdot 8}\frac{1}{k_1^2k_2^2k_3^2k_4^2}\Big(\delta^{ab}\delta^{cd} f_{\mathrm{S}}(1,2;3,4;\omega) + \delta^{ac}\delta^{bd} f_{\mathrm{S}}(1,3;2,4;\omega) + \delta^{ad}\delta^{bc} f_{\mathrm{S}}(1,4;2,3;\omega)\Big) \quad (2.3)$$

and

$$\varphi_{4\mathrm{A}}^{abcd} = -\frac{1}{3\cdot 8}\frac{1}{k_1^2k_2^2k_3^2k_4^2}\Big(f^{abm}f^{mcd} f_{\mathrm{A}}(1,2;3,4;\omega) + f^{acm}f^{mbd} f_{\mathrm{A}}(1,3;2,4;\omega) + f^{adm}f^{mbc} f_{\mathrm{A}}(1,4;2,3;\omega)\Big)\,. \quad (2.4)$$

Here f_{S} and f_{A} are ω-dependent, positive-valued functions which play the role of unintegrated gluon densities. Combining them with the quark loop expressions,

$$\Delta F_{T,L}^{\mathrm{R}} = -\frac{1}{128\omega\pi^2}\left(\frac{Q^2}{Q_0^2}\right) D_4^{\mathrm{R};abcd} \otimes \varphi_4^{abcd}(\omega)^{\tau=4}\,, \quad (2.5)$$

and retaining only those terms which give rise to Q^2-logarithms, we arrive at the following twist-4 corrections to the transverse and longitudinal structure functions:

$$\Delta F_T^{\mathrm{R}} = \frac{1}{64}\frac{\alpha_{\mathrm{s}}^2}{\pi^2}\sum_f e_f^2\,\frac{1}{\omega}\left(\frac{Q_0^2}{Q^2}\right)\frac{2}{5} \cdot\frac{1}{3}\left[14\varphi_{4\mathrm{S}}(\omega) - 9\varphi_{4\mathrm{A}}(\omega)\right] \quad (2.6)$$

and[1]

$$\Delta F_L^{\mathrm{R}} = -\frac{2}{64}\frac{\alpha_{\mathrm{s}}^2}{\pi^2}\sum_f e_f^2\,\frac{1}{\omega}\left(\frac{Q_0^2}{Q^2}\right)\left(\frac{94}{225} + \frac{4}{15}\ln\left(\frac{Q^2}{Q_0^2}\right)\right) \times\frac{1}{3}[14\varphi_{4\mathrm{S}}(\omega) - 9\varphi_{4\mathrm{A}}(\omega)]\,. \quad (2.7)$$

The ω-dependence of initial conditions $\varphi_{4\mathrm{S}}(\omega)$ and $\varphi_{4\mathrm{A}}(\omega)$ will be assumed to lead to a power-like behavior of the form $(1/x)^{2\lambda}$ where the exponent λ is unknown. Thus, together with the $1/Q^2$ suppression, these twist-4 corrections are of the form

$$\Delta F_{T,L} \sim \frac{Q_0^2}{Q^2}\left(\frac{1}{x}\right)^{2\lambda}\,. \quad (2.8)$$

From this general observation one immediately sees that the value of Q^2 where twist four becomes important is x-dependent. One of the most striking features is the sign structure: the transverse and longitudinal cross sections, (2.6) and (2.7), have opposite signs, and in $\Delta F_2 = \Delta F_T + \Delta F_L$ one faces a strong cancellation. If $\varphi_{4\mathrm{S}}$ and $\varphi_{4\mathrm{A}}$ are of the same order of magnitude (such that the square bracket expression is positive), we expect the twist-4 corrections

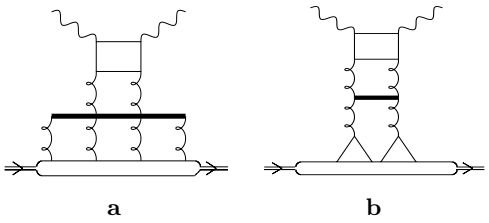

Fig. 2a,b. Corrections of order α_s

to F_2 being slightly dominated by the negative corrections to F_L, i.e. the higher twist corrections to F_2 could be small and negative.

It is important to note that these corrections to the deep inelastic structure functions are closely related to the twist-4 corrections to the cross section of diffractive $q\bar{q}$ production (the s-discontinuity line between gluon 2 and 3). Twist-4 in diffractive $q\bar{q}$ production has been observed experimentally, and it has to be a part of the twist-4 corrections to F_T or F_L. However, contrary to the most naive expectation, the two-gluon systems on both sides of this cutting line cannot be restricted to be in color singlet states: the AGK rules in perturbative QCD [5] require a structure of the form (2.2) and (2.3), and from this one easily sees that the system of gluons 1 and 2 is not restricted to color singlet.

Turning to corrections of the form $\alpha_s \ln Q^2/Q_0^2$ to Fig. 1 we face a mixing problem. In [3] it has been argued, on the basis of an all-order analysis in the double-logarithmic approximation, that there are several gluonic twist-4 operators, four-gluon operators and one two gluon operators. They have different Q^2-evolution equations, and they couple to the proton with different couplings. Furthermore, they mix, i.e. there are transitions from two-gluon states in the t-channel to four-gluon states. When computing $\alpha_s \ln Q^2/Q_0^2$ corrections to the diagrams in Fig. 1c, we group the contributions in the form shown in Fig. 2: (a) illustrates the transition of the two-gluon state to the four-gluon state and leads to the correction $\Delta F^{\rm I}$, and (b) illustrates the first evolution step of the two-gluon operator and gives the correction to $\Delta F^{\rm R}$. The calculation of these diagrams is described in [3] and leads to the following twist-4 contributions:

$$\Delta F_T^{\rm I} = -\frac{1}{16}\,\frac{\alpha_{\rm s}^3}{\pi^3}\sum_f e_f^2\,\frac{1}{\omega^2}\left(\frac{Q_0^2}{Q^2}\right)\ln\left(\frac{Q^2}{Q_0^2}\right)\frac{2}{5}\varphi_{4\rm S}(\omega), \quad (2.9)$$

$$\Delta F_L^{\rm I} = \frac{2}{16}\,\frac{\alpha_{\rm s}^3}{\pi^3}\sum_f e_f^2\,\frac{1}{\omega^2}\left(\frac{Q_0^2}{Q^2}\right)\left\{\frac{94}{225}\ln\left(\frac{Q^2}{Q_0^2}\right) + \frac{4}{15}\ln^2\left(\frac{Q^2}{Q_0^2}\right)\right\}\varphi_{4\rm S}(\omega)\,, \quad (2.10)$$

and

$$\Delta F_T^{\rm R} = \frac{1}{64}\,\frac{\alpha_{\rm s}^2}{\pi^2}\sum_f e_f^2\,\frac{1}{\omega}\left(\frac{Q_0^2}{Q^2}\right)\left(1+\frac{N_c\alpha_s}{\pi\omega}\ln\left(\frac{Q^2}{Q_0^2}\right)\right)\frac{2}{5} \cdot\frac{1}{3}[14\varphi_{4\rm S}(\omega) - 9\varphi_{4\rm A}(\omega)]\,, \quad (2.11)$$

$$\Delta F_L^{\rm R} = -\frac{2}{64}\,\frac{\alpha_{\rm s}^2}{\pi^2}\sum_f e_f^2\,\frac{1}{\omega}\left(\frac{Q_0^2}{Q^2}\right)\left\{\frac{94}{225}\left[1+\frac{N_c\alpha_s}{\pi\omega}\times\ln\left(\frac{Q^2}{Q_0^2}\right)\right] + \frac{4}{15}\left[\ln\left(\frac{Q^2}{Q_0^2}\right) + \frac{N_c\alpha_s}{\pi\omega}\times\ln^2\left(\frac{Q^2}{Q_0^2}\right)\right]\right\}\frac{1}{3}\left[14\varphi_{4\rm S}(\omega) - 9\varphi_{4\rm A}(\omega)\right]\,. \quad (2.12)$$

Note by the comparison of (2.11), (2.12) with (2.6), (2.7), respectively, that ΔF^R gets additional $\alpha_s \ln Q^2/Q_0^2$ corrections without changing the structure of initial conditions. The corrections ΔF^I are of the order α_S^2 ($\alpha_S \ln Q^2/Q_0^2$), thus they are not present in the lowest order result which is proportional to α_S^2.

For low Q^2-values it is not a priori clear whether these corrections to the twist-4 contributions are important or not: there is an additional suppression factor $\frac{N_c\alpha_s}{\pi}$, and for low Q^2-values the logarithm $\log Q^2/Q_0^2$ does not provides much enhancement. To get a first idea, it may, again, be useful to draw a connection with diffractive dissociation. As illustrated in Fig. 2a, these diagrams describe diffractive production of $q\bar{q}g$ systems. There is no doubt that these diffractive states have been observed at HERA: a direct analysis of their twist-4 component (e.g. the observation of diffractive final states with only hard jets) would provide a direct evidence for the presence of these higher twist corrections in the deep inelastic structure function.

A simple analysis of twist-4 corrections could be based upon the presented low-order expressions. However, even within this framework we need two initial conditions, ϕ_S and ϕ_A. Relating them to the twist-4 diffractive $q\bar{q}$ cross section (as described in [3]) gives only one condition, and, hence, is not enough. We are therefore lead to build a model for the initial conditions. The most successful description of the low-Q^2 transition region at HERA has been provided by the saturation model of [6], and we will use this model to determine the initial conditions.

3 Twist Four in the Saturation Model

Let us first briefly review the model of [6] and its decomposition into twist components. It is well known that the $\gamma^* p$-cross sections,

$$\sigma_{T,L}(x,Q^2) \;=\; \frac{4\pi^2\alpha_{em}}{Q^2}F_{T,L}(x,Q^2)\,, \quad (3.1)$$

can be written at small x as [8,9]:

$$\sigma_{T,L}(x,Q^2) \;=\; \int d^2\mathbf{r}\int_0^1 dz\,|\Psi_{T,L}(z,\mathbf{r})|^2\;\hat{\sigma}(x,r^2) \quad (3.2)$$

[1] We changed the definition of F_L in comparison to [3]. Now, F_L is twice the previous one to have $F_2 = F_T + F_L$

where $\Psi_{T,L}(z,\mathbf{r})$ denotes the transverse and longitudinally polarized photon wave functions, and $\hat{\sigma}(x,r^2)$ is the dipole cross section which describes the interaction of the $q\bar{q}$ pair with the proton. In addition, z is the momentum fraction of the photon carried by the quark, and r is the relative transverse separation between the quarks. The wave functions are solely determined by the coupling of the photon to the $q\bar{q}$ pair, see e.g. [9]. In [6] the dipole cross section is assumed to depend on x through the ratio of the transverse separation r and the saturation radius $R_0(x)$, and the following form is proposed:

$$\hat{\sigma}(x,r^2) = \sigma_0\, g\left(\frac{r^2}{4R_0^2}\right) \equiv \sigma_0\left\{1-\exp\left(-\frac{r^2}{4R_0^2}\right)\right\}. \quad (3.3)$$

At small r ($r \ll 2R_0$), the dipole cross section grows quadratically with r, $\hat{\sigma} \sim \sigma_0 r^2/4R_0^2$, while for large r ($r \gg 2R_0$), it saturates, $\hat{\sigma} = \sigma_0$. In order to describe the energy dependence both of the total DIS cross sections and of the low-Q^2 cross section measured at HERA, the saturation radius has the following x-dependent form:

$$R_0^2(x) \;=\; \frac{1}{Q_0^2}\left(\frac{x}{x_0}\right)^{\lambda} \quad (3.4)$$

with $Q_0 = 1$ GeV. Equations (3.2)-(3.4) define the saturation model. The physical motivation for such a parameterization and its significance for diffractive processes in DIS is discussed at length in [6,7]. The three parameters in the model are determined from a fit to the total DIS cross section data at $x < 0.01$ and look as follows: $\sigma_0 = 23$ mb, $x_0 = 3\cdot 10^{-4}$ and $\lambda = 0.29$. In this way a very good description of data in a broad range of Q^2 and x is obtained. In fact there is a fourth parameter in the model, an effective quark mass $m_f = 140$ MeV in the photon wave function, chosen such that the results of the model, extended down to photoproduction region, are in a good agreement with photoproduction data measured at HERA.

In order to evaluate the cross section (3.2) it is convenient to employ the Mellin transform to factorize the wave function from the dipole cross section:

$$\begin{aligned}\sigma_{T,L}(x,Q^2) &= \int_{-\infty}^{\infty}\frac{d\nu}{2\pi}\int d^2\mathbf{r}\int_0^1 dz|\Psi_{T,L}(z,\mathbf{r})|^2 \\ &\quad\times\int\frac{dr'^2}{r'^2}\left(\frac{r}{r'}\right)^{1+2i\nu}\hat{\sigma}(x,r'^2) \\ &= \sigma_0\int_{-\infty}^{\infty}\frac{d\nu}{2\pi}\left(\frac{1}{Q^2R_0^2(x)}\right)^{1/2+i\nu} \\ &\quad\times H_{T,L}\left(\nu,\frac{m_f^2}{Q^2}\right)G(\nu)\,. \end{aligned} \quad (3.5)$$

In the case of zero quark mass we obtain

$$\begin{aligned}H_T(\nu,0) &= \frac{6\alpha_{em}}{2\pi}\sum_f e_f^2\,\frac{\pi}{16}\,\frac{9/4+\nu^2}{1+\nu^2}\left(\frac{\pi}{\cosh(\pi\nu)}\right)^2 \\ &\quad\times\frac{\sinh(\pi\nu)}{\pi\nu}\,\frac{\Gamma(3/2+i\nu)}{-\Gamma(-1/2-i\nu)}\end{aligned} \quad (3.6)$$

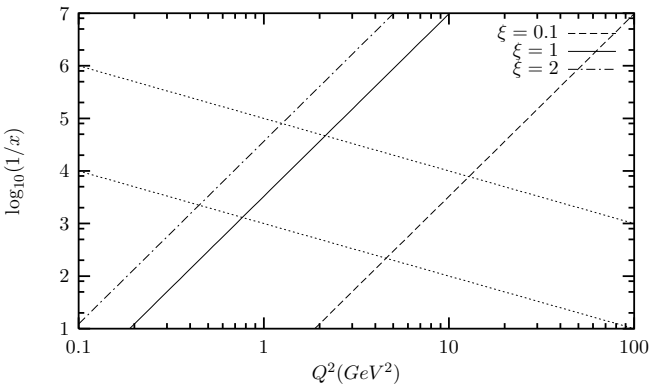

Fig. 3. The solid line ($\xi = 1$) in the (x,Q^2) plane indicates a critical line of the model [6]. The area between the two dotted lines corresponds to the acceptance region of HERA

and

$$\begin{aligned}H_L(\nu,0) &= \frac{6\alpha_{em}}{2\pi}\sum_f e_f^2\,\frac{\pi}{8}\,\frac{1/4+\nu^2}{1+\nu^2}\left(\frac{\pi}{\cosh(\pi\nu)}\right)^2 \\ &\quad\times\frac{\sinh(\pi\nu)}{\pi\nu}\,\frac{\Gamma(3/2+i\nu)}{-\Gamma(-1/2-i\nu)}.\end{aligned} \quad (3.7)$$

In addition, $G(\nu)$ in (3.5) equals:

$$G(\nu) = \int_o^{\infty} d\hat{r}^2\left(\hat{r}^2\right)^{-3/2-i\nu} g(\hat{r}^2) = -\Gamma(-1/2-i\nu), \quad (3.8)$$

for the saturation form of the dipole cross section $g(\hat{r}^2) = 1-e^{-\hat{r}^2}$. From relation (3.5) we see that the cross sections $\sigma_{T,L}$ depend on x in the saturation model only through the combination

$$\xi \;\equiv\; \frac{1}{Q^2R_0^2(x)} \;=\; \frac{Q_0^2}{Q^2}\left(\frac{x_0}{x}\right)^{\lambda}. \quad (3.9)$$

Notice that a similar combination, (2.8), occurs in the twist-4 analysis in the previous section.

The detailed discussion in [6] (which will not be repeated here) shows that there is an essential change in the energy (and also Q^2) dependence of the cross section if we move from the "perturbative" region, $\xi < 1$ (large Q^2 and not too small x), to the nonperturbative "Pomeron" region, $\xi > 1$ (small Q^2 and very small x). In the former region we have a power-like rise in $1/x$ (in agreement with the observed rise of the structure function at small x), whereas in the latter one the cross section stays constant (apart from a logarithmic enhancement factor). Hence the region $\xi \approx 1$ (see Fig. 3) marks the transition from one region to the other. In the region $\xi < 1$ it is natural to expand the inclusive cross sections in powers of ξ (which means powers of $1/Q^2$) while in the region $\xi > 1$ in powers of $1/\xi$ or Q^2. It is clear, however, that the expansion in powers of $1/Q^2$ cannot be valid down to $Q^2 = 0$. Therefore, approaching the transition region $\xi \approx 1$ from the perturbative side one expects the leading-ξ approximation to fail somewhat to the right of the line $\xi = 1$ (called a critical line in [6]).

With expressions (3.5)-(3.9) the above discussion can be made more precise. The expansion in powers of ξ will be identified as "twist expansion" (below we will explain why). The power series in ξ (or $1/\xi$) is determined by the singularities of the integrand in (3.5) in the complex ν-plane. These are single or multiple poles, located at $\nu = \pm i(2n+1)/2$ with $n = 0, 1, 2, ...$

The ν-integration runs along the real axis, and for $\xi < 1$ it is tempting to close the contour in the lower half-plane. A closer look reveals that in such a case an asymptotic expansion for our cross sections is constructed. This is done by computing residues of the poles in the lower half-plane which leads to an expansion in powers of ξ or $1/Q^2$. Now, the critical line (or better, a strip) indicates a limit on validity of the asymptotic twist expansion. It is also possible to close the contour in the upper half-plane in which case a convergent expansion in positive powers of $1/\xi$ or Q^2 is obtained for any value of $\xi \neq 0$, ∞[2]. However, this expansion is not practical in the large Q^2 or small ξ analysis.

The first singularity encountered in the lower plane is a pole at $\nu = -i/2$. In the saturation model the transverse cross section has a double pole which generates a logarithmic behavior for the leading-twist contribution:

$$\sigma_T = \sigma_0 \sum_f e_f^2 \frac{\alpha_{em}}{\pi} \left(\frac{7}{6}\xi - \psi(2)\xi + \xi \ln(1/\xi) \right). \quad (3.10)$$

The longitudinal leading-twist contribution has only a single pole and therefore does not produce a logarithm:

$$\sigma_L = \sigma_0 \sum_f e_f^2 \frac{\alpha_{em}}{\pi} \xi. \quad (3.11)$$

Higher-twist contributions can be obtained by evaluating the residues at the lower lying poles, the twist-4 contribution at the pole $\nu = -3i/2$, etc. The results for the transverse contributions are:

Twist-4:

$$\sigma_T = \sigma_0 \sum_f e_f^2 \frac{\alpha_{em}}{\pi} \frac{6}{10}\xi^2, \quad (3.12)$$

Twist-6:

$$\sigma_T = \sigma_0 \sum_f e_f^2 \frac{\alpha_{em}}{\pi} \left(\frac{43}{1225}\xi^3 - \frac{12}{35}\psi(4)\xi^3 + \frac{12}{35}\xi^3 \ln(1/\xi) \right), \quad (3.13)$$

Twist-8:

$$\sigma_T = \sigma_0 \sum_f e_f^2 \frac{\alpha_{em}}{\pi} \left(-\frac{262}{11025}\xi^4 + \frac{4}{35}\psi(5)\xi^4 - \frac{4}{35}\xi^4 \ln(1/\xi) \right). \quad (3.14)$$

[2] We thank Lech Mankiewicz for a discussion on this point

For the longitudinal contributions we find:

Twist-4:

$$\sigma_L = \sigma_0 \sum_f e_f^2 \frac{\alpha_{em}}{\pi} \times \left(-\frac{94}{75}\xi^2 + \frac{4}{5}\psi(3)\xi^2 - \frac{4}{5}\xi^2 \ln(1/\xi) \right), \quad (3.15)$$

Twist-6:

$$\sigma_L = \sigma_0 \sum_f e_f^2 \frac{\alpha_{em}}{\pi} \times \left(\frac{654}{1225}\xi^3 - \frac{36}{35}\psi(4)\xi^3 + \frac{36}{35}\xi^3 \ln(1/\xi) \right), \quad (3.16)$$

Twist-8:

$$\sigma_L = \sigma_0 \sum_f e_f^2 \frac{\alpha_{em}}{\pi} \left(-\frac{1636}{18375}\xi^4 + \frac{48}{175}\psi(5)\xi^4 - \frac{48}{175}\xi^4 \ln(1/\xi) \right). \quad (3.17)$$

It is not surprising to see a strong similarity between the twist-4 contributions (2.6) and (2.7) computed to lowest order in QCD, and those found in the saturation model (3.12) and (3.15). In particular, the sign structure is the same: σ_T is positive while σ_L is negative. Also, σ_L contains a logarithm while σ_T does not. Finally, the ratio of the twist-4 contributions,

$$\frac{\sigma_L}{\sigma_T} = -\frac{94/75 + 4/5\,(\ln(1/\xi) - \psi(3))}{3/5}, \quad (3.18)$$

is similar to the ratio obtained from the lowest order QCD calculation

$$\frac{\Delta F_L^R}{\Delta F_T^R} = -\frac{94/75 + 4/5 \ln(Q^2/Q_0^2)}{3/5}. \quad (3.19)$$

Thus, the saturation model can be interpreted as a result of summing the diagrams shown in Fig. 1a and 1c (and more "iterations of gluon ladders"): the leading twist comes entirely from Fig. 1a, twist four from Fig. 1c etc. Viewed in this way, the model can be used to define values of the initial conditions for (2.6) and (2.7), but only in the combination $14\varphi_{4S} - 9\varphi_{4A}$. The higher order corrections illustrated in Fig. 2a are not included in the model. The success of the model might indicate that this type of corrections is not very important near the transition (critical) line; but it may also be that a suitable modification of the model might be necessary.

4 Numerical analysis

Further insight will be gained through a numerical study. We choose to use the expressions of Sect. 3 and compare the full expressions (3.5) (with $m_f = 0$), which can be integrated numerically, with the twist-expansion (3.10)-(3.17).

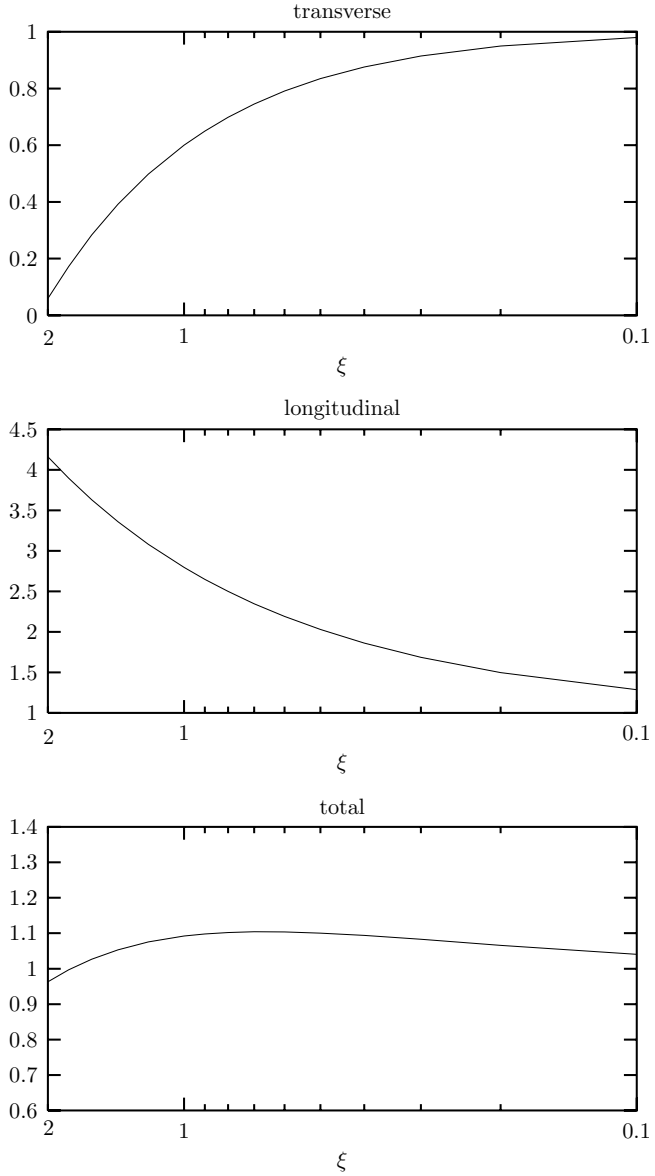

Fig. 4. The ratio of the leading-twist and the exact cross section in the saturation model: for the transverse, $\sigma_T^{\tau=2}/\sigma_T$, longitudinal, $\sigma_L^{\tau=2}/\sigma_L$, and the total, $\sigma_{T+L}^{\tau=2}/\sigma_{T+L}$, cross sections

As far as the twist-4 terms alone are concerned, we could have started from the saturation model, extract the initial conditions and than turned to the QCD approximations listed in Sect. 2. For our present discussion, however, we find it more instructive to study the role of higher twist (in particular, twist-4) in a more general context. The saturation model, which describes the data, provides an analytical formula for the cross sections and allows to investigate the twist expansion and its breakdown near $\xi = 1$. Since the dependence upon Q^2 and x is through the variable ξ, we present the numerical results as a function of ξ.

In Fig. 3 we show lines of constant ξ ($\xi = 2,\ 1,\ 0.1$): variation of ξ means moving from one line to another. With the help of Fig. 3 ξ can be translated into the x and Q^2 variables. We begin with presenting the ratios of the leading-twist approximations to the full cross sections as a function of ξ. In Fig. 4 we show the ratios for the transverse $\sigma_T^{\tau=2}/\sigma_T$, longitudinal $\sigma_L^{\tau=2}/\sigma_L$, and the total $(\sigma_L^{\tau=2} + \sigma_T^{\tau=2})/(\sigma_T + \sigma_L)$, cross sections. The striking result is that for both the transverse and longitudinal cross sections separately the higher twist corrections become large when we are approaching the transition line $\xi = 1$. Moreover, the transverse higher twist correction is positive while the longitudinal one is negative. In the sum, however, those corrections almost cancel each other and the overall correction is small.

Table 1. The MRST values of the higher-twist coefficient $D_2(x)$ in (4.1)

x	$D_2(x)(GeV^2)$
0-0.0005	0.0147
0.0005-0.005	0.0217
0.005-0.01	-0.0299
0.01-0.06	-0.0382
0.06-0.1	-0.0335
0.1-0.2	-0.121
0.2-0.3	-0.190
0.3-0.4	-0.242
0.4-0.5	-0.141

This is a possible explanation of the smallness of the higher twist correction to F_2 found in the analysis of MRST [10]. The authors of this analysis use the following simple parameterization:

$$F_2^{HT}(x,Q^2) = F_2^{LT}(x,Q^2)\left(1 + \frac{D_2(x)}{Q^2}\right), \qquad (4.1)$$

and determined the function $D_2(x)$ from a fit to DIS data. The result is given in Table 1 which we reproduce from [10]. In general, for small x, $D_2(x)$ is small and negative but it becomes positive for the smallest x. We found a similar result, the leading twist approximation deviates from the exact formula by less than 10%. The sign structure of this deviation also agrees with the MRST analysis; it is negative but to the left of the transition line the deviation becomes positive. The last result should be taken with some care since, strictly speaking, the twist expansion for $\xi > 1$ in the saturation model makes no longer sense, and a new expansion in powers Q^2 is appropriate. We extrapolated, however, the leading twist formula to that region and found an agreement with the exact result up to $\xi = 2$. This indicates that the phenomenological success of a leading-twist analysis might be deceptive: the leading-twist approximation to F_2 remains a good approximation also in the region in which the whole twist expansion has already collapsed.

The last point is also illustrated in Fig. 5 where the individual higher twist components are shown. We plot $\sigma_T^\tau + \sigma_L^\tau$ for $\tau = 2, 4, 6, 8$, together with the exact result (solid line). The overall impression is that near $\xi = 1$ all higher twist corrections are getting large, leading to the

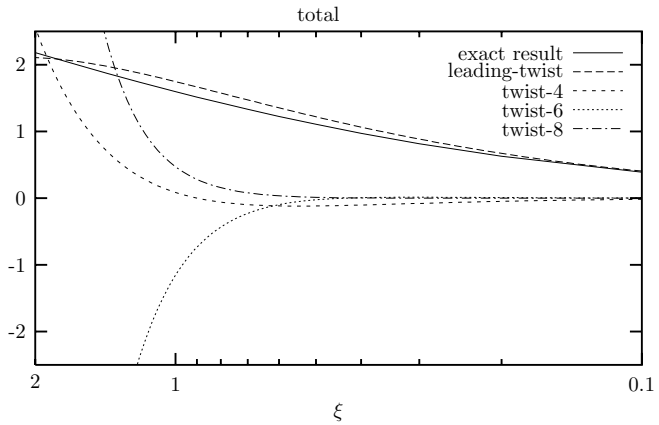

Fig. 5. The exact total cross section (solid line) and the higher twist contributions in the saturation model as a function of the parameter ξ defined in the text. The cross sections are rescaled by a common factor

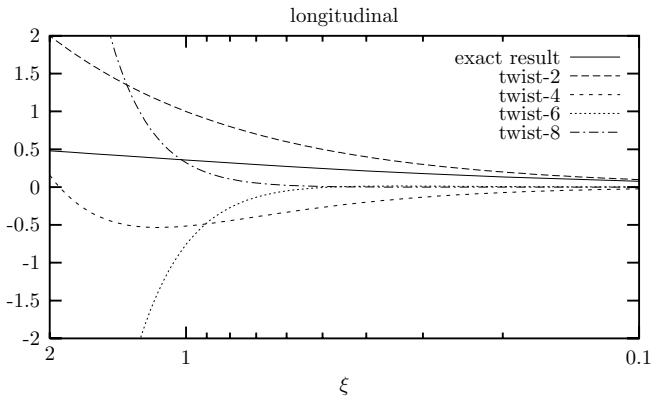

Fig. 7. The exact longitudinal cross section (solid line) and the higher twist longitudinal contributions in the saturation model as a function of the parameter ξ. The cross sections are rescaled by a common factor

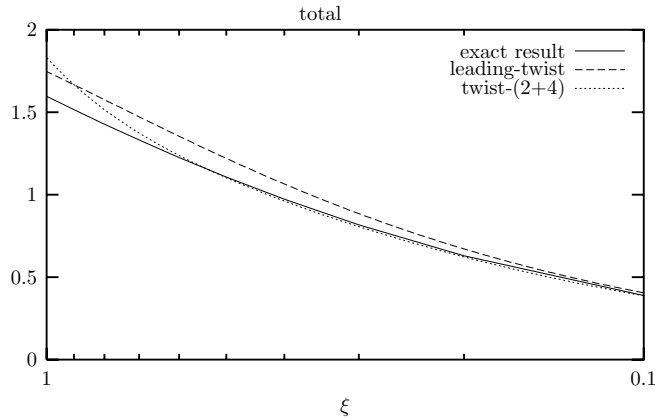

Fig. 6. The same as in Fig. 5 but with the leading twist and twist-4 added (dotted line)

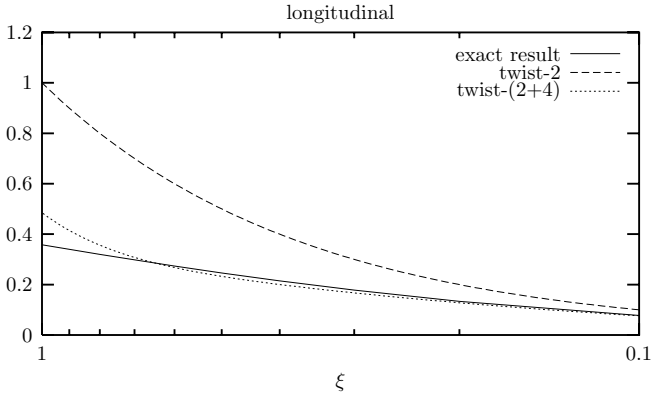

Fig. 8. The same as in Fig. 7 but with the leading twist and twist-4 added (dotted line)

conclusion that the concept of higher twist becomes meaningless. If we naively extrapolate the higher twist formulas to the region $\xi > 1$ they diverge. Nevertheless, to the right of $\xi = 1$ there is a region where twist 6 and 8 are small and can be neglected, whereas twist-4 accounts for the deviation between the twist-2 approximation and the exact result. Figure 6 illustrates this in another way: the sum of twist-2 and twist-4 provides a rather accurate description of the exact formula. In this region (in Fig. 3 between the two lines $\xi = 0.2$ and $\xi = 0.9$) twist-4 corrections should improve the QCD description of deep inelastic scattering.

In Fig. 7 we present the results of the analysis performed only for the longitudinal twist contributions σ_L^τ and $\tau = 2, 4, 6, 8$. The striking result in comparison to the total cross section analysis is a large and negative twist-4 contribution which accounts for a large difference between the exact and leading twist result. This is shown in Fig. 8: again the sum of twist-2 and twist-4 provides an accurate description of the exact formula. Notice that the difference $\sigma_L^{\tau=2} - \sigma_L^{exact}$ is large already at $\xi = 0.1$. Taking this result, we conclude that an analysis of the longitudinal structure functions F_L based entirely on the leading twist result is unreliable already for quite high values of Q^2 and not to small x. A similar effect, although not so pronounced, occurs for the transverse cross section (large twist-4 corrections for the transverse case were also discussed in [11]). The role of higher twist in the longitudinal structure function was broadly studied in [14] and a qualitatively similar results to ours were obtained there for small x.

In summary, the main lesson to be learned from this study is the cancellation of higher twist in F_2: twist-4 is not small, neither in the transverse nor in the longitudinal part, but it is hardly visible in the sum of both because of the mutual cancellation. Moreover, the twist-2 approximation to F_2 works even beyond $\xi = 1$ where the whole concept of a twist expansion should make no sense. As far as F_L is concerned, the leading twist significantly exceeds the exact result for $\xi > 0.1$, and a large and negative twist-4 correction is necessary to obtain an agreement with the exact result.

5 Discussion and conclusions

In this article we have carried out a simple numerical analysis of gluonic twist-4 corrections in the low-Q^2, small-x HERA region. We have reviewed what an analysis of lowest-order QCD diagrams suggests. One of the most striking features are differences in sign between transverse and longitudinal twist-4 corrections which may lead to a small twist-4 correction, even if the corrections to F_T or F_L are not small at all. Because of the unknown initial conditions more input is needed. We then have used the saturation model which provides an excellent description of both F_2 and the DIS diffractive cross section at HERA, and we have analyzed its higher twist content. We found a one-to-one correspondence between the twist expansion of this model and the QCD diagrams discussed before. The model can therefore be used to define initial conditions of a QCD higher twist analysis.

In our numerical analysis we have restricted ourselves to a careful study of the saturation model. We found that, indeed, twist-4 corrections to F_2 remain small, and this smallness is due to an almost complete cancellation between large corrections to F_T and F_L. This implies that although twist four corrections are small in F_2, the use of the leading-twist DGLAP formalism for extracting structure functions becomes doubtful in the low-Q^2, small-x HERA region. Within the saturation model we have quantified the limit of applicability.

This problem is even more acute for F_L alone, where the large twist-4 correction is directly exposed, providing a crucial contribution which brings the leading twist result close to the exact one. The DGLAP formalism might not be reliable in this case even for higher values x and Q^2, see Fig. 8.

Clearly, our numerical conclusions are based upon a specific model. The phenomenological success of this model provides some reasons to believe that the conclusions are realistic. Moreover, on a qualitative level our conclusions are in agreement with the independent fit to the HERA data of [10]. Nevertheless, some uncertainty remains. We have outlined that in the saturation model some contributions are not present which one would expect to see when starting from QCD diagrams. If included they may modify the subtle balance between transverse and longitudinal structure function. They may also shift the transition region (the "transition line" of the saturation model, in reality, may turn out to be a rather narrow "transition strip"). However, the coincidence with the MRST fit makes us feel that the conclusions of our analysis are "not far from reality".

References

1. R.K. Ellis, W. Furmanski, R. Petronzio, Nucl. Phys. **B 212** (1983) 29
2. A.B. Bukhvostov, G.V. Frolov, L.N. Lipatov, E.A. Kuraev, Nucl. Phys. **B 258** (1985) 601
3. J. Bartels, C. Bontus, Phys. Rev. **D 61** (2000) 034009
4. J. Bartels, C. Bontus, H. Spiesberger, preprint DESY-99-068, hep-ph/9908411
5. J. Bartels, M.G. Ryskin, Z. Phys. **C 76** (1997) 241
6. K. Golec-Biernat, M. Wüsthoff, Phys. Rev. **D 59** (1999) 014017
7. K. Golec-Biernat, M. Wüsthoff, Phys. Rev. **D 60** (1999) 114023
8. N.N. Nikolaev, B.G. Zakharov, Z. Phys. **C 49** (1990) 607
9. J.R. Forshaw, D.A. Ross, QCD and the Pomeron, Cambridge University Press, 1997
10. A.D. Martin, R.G. Roberts, W.J. Stirling, R.S. Thorne, Phys. Lett. **B 443** (1998) 301
11. A.D. Martin, M.G. Ryskin, Phys.Lett. **B 431** (1998) 395
12. J. Bartels and M. Wüsthoff, Z. Phys. **C 66** (1995) 157
13. J. Bartels, Phys. Lett. **B 298** (1993) 204, Z.Phys. **C 60** (1993) 471
14. B. Badelek, J. Kwiecinski and A. Stasto, Z. Phys. **C 74** (1997) 297, A. Stasto, Acta Phys. Polon. **B 27** (1996) 1353